Self-diffusion in granular shear flows

By CHARLES S. CAMPBELL

Department of Mechanical Engineering, University of Southern California,
Los Angeles, CA 90089-1453, USA

The collisionally induced random particle velocities in a rapid granular shear flow drive the diffusion of particles in manner directly analogous to the thermal diffusion of molecules or the eddy-induced diffusion in a turbulent flow. This paper reports measurements, via computer simulation, of the anisotropic diffusion tensor for a granular shear flow. The components are determined both by particle tracking and through velocity correlations, which are found to agree with reasonable accuracy. As might be expected from symmetry arguments, there are four non-zero components generated in a simple shear flow: the three diagonal components and one off-diagonal component.

1. Introduction

Powders must frequently be mixed together before any sort of processing can begin. The importance of this area can be ascertained from the review articles by Fan & Chen (1990) and Poux *et al.* (1990). The problem is hampered by that tendency of dissimilar materials to experience flow-induced segregation – a byproduct of exactly the same flow processes that are supposed to bring about mixing. The mixing of similar particles is important in other transport problems; for example, Wang & Campbell (1992) showed that the internal transport of heat in a shearing granular material is a byproduct of the mixing of hot and cold particles. On a microscopic scale, the mixing of granular materials is accomplished by the motion of particles relative to one another. If a particle is to move relative to its neighbours, first a void must open that is large enough for the particle to move into, and secondly, there must be relative velocity that induces the particle to fill that void. Thus, the mixing of granular materials is a flow-induced phenomenon as, obviously, neither event could take place in a static granular bed.

On a microscopic scale, the phenomena required are brought about by the flow-induced random motion of the granules. These random motions are so reminiscent of the thermal motion of molecules in the kinetic theory of gases that their mean-square magnitude is commonly referred to as the 'granular temperature'. The random velocities both move particles apart to create a void and provide the impetus for a particle to move into and fill that void. Consequently, the rate at which these processes occur will depend on the magnitude of the granular temperature. However, the granular temperature is itself a byproduct of the local flow field and its magnitude depends on both flow and particle properties. Naturally, the particle concentration will also have a strong effect on the probability of opening a void and one expects significantly smaller mixing rates at large values of the particle concentration.

This problem has received some experimental attention. Buggish & Löffelmann (1989) studied granule mixing in a two-dimensional granular shear cell. A portion of

their test material was coloured and formed into an inner ring of the cell. The shear cell was then started and the mixing observed from the changes in the local concentration of the coloured particles. Hsiau & Hunt (1992) and Natarajan, Hunt & Taylor (1995) studied the flow of layers of differently coloured glassbeads down a vertical channel and, in a similar manner, observed the mixing of the streams. Zik & Stavans (1991) studied the dispersion of a strip of coloured beads in a vibrationally excited system. All three found that the concentration distribution could be fitted to the results of a diffusion equation and concluded that granular mixing is a diffusion process. Scott & Bridgwater (1976) and Bridgwater (1980) studied self-diffusion near close-packed conditions in an unsteady linear shear device. Finally, Savage (1993) and Savage & Dai (1993) have produced a simple theory for the process which is supported by limited computer simulations.

Γ This paper describes measurements of diffusion coefficients in a computer simulation of simple shear flows of a granular material composed of uniform-sized spheres. All of the above experiments were limited to observing the diffusion in only one direction, usually the direction parallel to their velocity gradient. But a computer simulation can observe the diffusion in all possible directions. Furthermore, as the granular temperature is not isotropically distributed (see Campbell 1989, 1990) one expects anisotropic diffusion, i.e. the largest diffusion should occur in the directions with the largest granular temperature. Thus, instead of a single diffusion coefficient, a tensor of coefficients, $\boldsymbol{D}$, is required to properly model the diffusion process, such that the diffusive flux, $\boldsymbol{\Gamma}$, is related to a concentration gradient, ∇c, by the formula

$$\boldsymbol{\Gamma} = \boldsymbol{D} \cdot \nabla c, \tag{1}$$

where the component D_{ij} represents the coefficient of diffusion in the i-direction due to a concentration gradient in the j-direction. The use of a computer simulation permits the simultaneous measurement of all the components of $\boldsymbol{D}$.

Preliminary reports of this work appear in Campbell, Zhang & Cleary (1991) and Campbell & Zhang (1991).

2. Computer simulation

Other than the statistics that are gathered, the simulation used for this study is identical to that used to make stress tensor measurements by Campbell (1989). For general information on granular simulations, please refer to the reviews by Campbell (1986, 1997). Throughout the simulation, spherical particles (of mass m and radius R) are confined within a control volume of dimension L in the x-direction, H in the y-direction and B in the z-direction, such as that shown schematically in figure 1. (Here and in the following discussion, the x-direction will refer to the direction of mean motion. The boundaries of the system generate a mean-field velocity gradient in the y-direction. The z-direction refers to the coordinate out of the shear plane.) All of the sides of the control volume are bounded by 'periodic' boundaries: as a particle passes through one periodic boundary it re-enters through the opposite one with exactly the same position and relative velocity with which it left. This type of boundary gets its name because it simulates a situation in which the control volume and its particles are periodically repeated, infinitely many times, upstream, downstream, above, below, and beside, the central control volume. This set-up greatly enhances the computational efficiency of the simulation by permitting the simulation of an infinite volume while limiting the number of particles to the finite number initially placed in the control volume. It has the drawback that it is only applicable to flows with no gradients in the
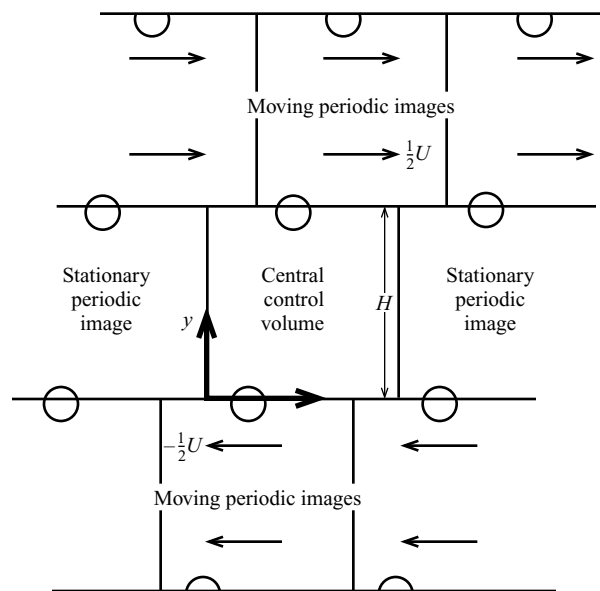
FIGURE 1. A schematic of the computer simulation control volume.

flow direction (i.e. steady, unidirectional flows). To impose a shear rate $\gamma = U/H$, the periodic images that bound the top and bottom of the control volume are set in motion with velocities $\frac{1}{2}U$ and $-\frac{1}{2}U$, respectively, in the x-direction. That is, when a particle exits the bottom of the central control volume, it re-enters the top with its x-direction velocity increased by U and a displaced x-coordinate that reflects the displacement of the origin of the moving periodic image. The opposite path is followed by particles that exit through the top of the control volume. With this set-up, uniformly shearing flows are assured. This simulation scheme was first used in molecular dynamics studies by Lees & Edwards (1972). Most of the current work was performed on control volumes of 216 particles which were originally arranged in a $6 \times 6 \times 6$ (referring to the x-, y- and z-directions) array. The particles are initially organized in a triangular prismatic packing, i.e. they are arranged in lines in the x-direction and these lines are organized in a triangular pattern in the (y, z)-plane. This corresponds to the shear-induced microstructure observed in molecular dynamics simulations by Heyes (1986). These lines are allowed to move with minimal interference from their neighbours and permit a shear flow at concentrations up to at least 60 % by volume. In most cases, the diffusion of particles soon breaks up the initial configuration. However, at very large concentrations, the particles cannot break out of the initial structure and the material exhibits non-diffusive behaviour.

The particles interact by colliding with one another. Each collision is assumed to occur instantaneously once the particle surfaces come into contact (this is essentially the hard-sphere approximation often used in the kinetic theory of gases and first used in molecular dynamics simulations by Alder & Wainwright (1959) and the collision result is computed from a standard centre-of-mass collision solution. The particles both translate and rotate. Dissipation is introduced through a coefficient of restitution, ϵ and a surface friction coefficient μ ($\mu = 0.5$ is used throughout). The collisional scheme is identical to that used in two dimensions by Campbell (1993) and the reader is referred there for more details.

After the initial configuration and velocities of the particles and boundaries are chosen, the simulation is allowed to proceed as it will , with no outside intervention, until it converges to a steady state. (For these simulations, a converged state was assumed to occur when the total system kinetic energy achieves nearly constant values. However, like all small thermodynamic systems, the kinetic energy will fluctuate slightly with time, making the determination of convergence somewhat difficult). Starting from the initial state, convergence was achieved after as little as 500 collisions per particle for most of these simulations, although they were typically run for over 1100 collisions per particle before statistics were gathered. The averaging period covered at least 8000 collision per particle, but for some cases, at large concentrations where collisions are frequent, it was extended to as much as 40 000 collisions per particle.

3. Particle diffusion

As stated in the Introduction, diffusion results from the random motions of the constituent particles that are reflected in the granular temperature. Now, there are two mechanisms that lead to temperature generation. The first is directly related to collisions as any collision between particles – even two particles that initially move with exactly the mean velocities appropriate to their positions – will result in the generation of random components of velocity. The direction of the collisionally induced velocity change depends on the geometry of the collision and will, thus, in the large, be randomly distributed. The second mode of temperature generation is, itself, a byproduct of the random particle velocities. Following its random path, a particle moving parallel to the local velocity gradient will pick up an apparently random velocity that is roughly equal to the difference in the mean velocity between its present location and the point of its last collision. Note that, like the first mode of temperature generation, the magnitude of the random velocities so generated will also be proportional to the local velocity gradient. However, unlike the collisional temperature generation, this 'streaming' mechanism can only generate one component of random velocity – the component that lies in the direction perpendicular to the mean velocity gradient (which, in this case, is the x-direction). Consequently, the granular temperature will be anisotropic with its largest component in the direction of mean motion. (This may be clearly seen in the results of Campbell 1989.) One might then expect to find the largest diffusivity in the direction of flow (D_{xx}).

As the collisions between particles dissipate energy, the granular temperature cannot be self-sustaining. Thus, the energy of the random motion can only come from the mean motion – that is, from the imposed shear flow – through the mechanisms described in the last paragraph. One can imagine an internal energy flow beginning with the energy of the imposed motion; part of that energy is converted to granular temperature through the mechanism of shear work only to eventually be dissipated away to real heat by the inelasticity of the collisions. (For more details on the energy flow patterns, see the discussion in the review article by Campbell 1990.) Thus, one expects a relationship between the granular temperature and the shear rate. This is represented by the dimensions parameter, S (which is the same as the 'R'-parameter defined by Savage & Jeffrey 1979), which is plotted in figure 2 and defined as

$$S = 2R\gamma/T^{1/2}. \tag{2}$$

(Note: the temperature, T, is defined as the mean-square average of the fluctuating velocity components: $T = \langle u_i' u_i' \rangle$. In this paper, it includes only the translational
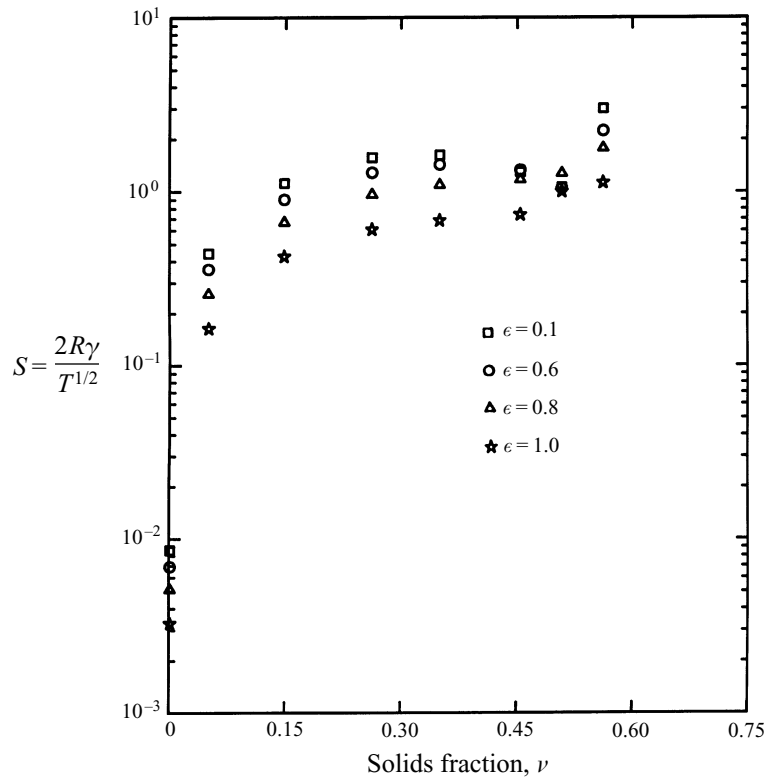
$$S = \frac{2R\gamma}{T^{1/2}}$$

FIGURE 2. The parameter S, plotted as a function of the solids fraction, ν.

components of the random velocity and not the rotational components.) One obvious feature of this curve is that the larger the coefficient of restitution, ϵ, the smaller the value of S, indicating a larger relative value of the granular temperature. This reflects the fact that the larger the coefficient of restitution, the smaller the rate of dissipation of the energy associated with the random particle velocities, resulting in correspondingly larger temperatures. Also, for small values of the solids fraction ν, the value of S is small, indicating that the granular temperature, T, is large compared to $(2R\gamma)^2$, but for most of the range of the solid fraction S is or order one, indicating that the two are of the same magnitude. The rapid decline in S as $\nu \to 0$ can be understood as follows: as mentioned before, the granular temperature is a result of shear work, which, in the simple shear configuration, is represented by $\tau_{xy}\gamma$. At such low densities the shear stress is generated by the 'streaming mechanism' (see, for example, Campbell 1989) in which the shear stress takes the form of a Reynolds' stress, $\tau_{xy} = \rho\langle u'v'\rangle$, where $\rho = \rho_p \nu$ is the local density (here ρ_p is the density of the solid material) and $\langle u'v'\rangle$ is the average of the fluctuating velocity components in the x- and y-directions respectively. Thus, the generation of granular temperature is proportional to the solids fraction, ν. Now, the dissipation of granular temperature is proportional to the collision rate, which, in turn, is proportional to the probability of finding two particles in contact. At small concentrations where the position of one particle has an insignificant effect of the position of any other, the probability of finding a particle at any location is proportional to ν, and, consequently, the probability of finding two particles in contact is proportional to ν^2. As a result, the ratio of generation to dissipation of granular temperature is proportional to $1/\nu$ and goes to infinity as $\nu \to 0$.

Thus, the granular temperature must diverge to infinity as the solid fraction is reduced, and, consequently, $S \to 0$ as $\nu \to 0$. This is clearly the case for the data plotted in figure 2. The lowest-concentration points plotted here correspond to $\nu = 0.001$, indicating that the divergence occurs very rapidly. (Note that this behaviour is a byproduct of the assumption that the only energy dissipation comes about from the inelasticity of the particles. Any other dissipation mechanism, such as drag from an interstitial fluid, would severely curtail this divergent behaviour). As a result, one expects huge diffusivities at small concentrations as, not only do the particles have a large free range of motion, but their random velocities divergently approach infinity. However, at moderate to large densities, like those commonly found in a granular flow the relative velocities due to the shear rate and the granular temperature will be of roughly the same magnitude and the mean free path of the particles will be less than a particle diameter, leading to dramatically smaller diffusivities.

There are two methods by which the components of the diffusion tensor may be determined. The first is by tracking the movement of the particles relative to their initial position, while taking into account the displacement due to the mean shear flow. The second is to borrow techniques from turbulent diffusion which relate the diffusivities to correlations of the random particle velocities. Both techniques were used in this investigation and will be discussed separately in the sections that follow.

3.1. *Measurement by particle tracking*

In essence, one can imagine choosing a particle and moving along with the mean velocity appropriate to its position in the flow. If one then traced the path followed by the particle, one would see it move away from its initial position following a random walk. If Δx_i is used to represent the displacement of a particle in the *i*-direction after a time Δt, then, if a system exhibits diffusive behaviour, one expects that over large Δt

$$\langle \Delta x_i \Delta x_j \rangle = 2 D_{ij} \Delta t, \tag{3}$$

where D_{ij} is the corresponding diffusion coefficient. Thus, the diffusion coefficient may be, in principle, computed from tracking the displacement of particles relative to their initial position. There are two exceptions to the law given by equation (3). The first is over extremely short times in which the particle velocities do not deviate far from their initial values. In that case, $\Delta x_i = u_i' \Delta t$ and $\Delta x_j = u_j' \Delta t$, where u_i' and u_j' represent the difference between the instantaneous velocity of a particle and the mean velocity appropriate to its location in the flow field. Thus

$$\langle \Delta x_i \Delta x_j \rangle = \langle u_i' u_j' \rangle (\Delta t)^2 \tag{4}$$

for small Δt.

The second exception occurs in the presence of a mean velocity field, such as the shear flow that exists in these simulations. As a particle follows its random path, it will move parallel to the velocity gradient into a region with a different mean velocity. Consequently, if one were to sit at the initial position of a particle and watch it diffuse away, one would observe it to be picked up and carried by the mean velocity field. Such a diffusion/velocity-field interactions was studied by Taylor (1953, 1954 *a, b*) to explain apparently anomalous behaviour for pipe flows and has since become known as 'Taylor dispersion'. As the mean motion can only augment the diffusion of particles in the direction of mean motion, (the *x*-direction in this case), only the D_{xx} components will be affected. On the practical side, this means that the mixing in the direction of flow is improved simply as a byproduct of the state of motion.

The effect of the mean shear motion on the apparent diffusion rate may be simply

understood if one realizes that the process occurs in two steps: (i) the particle diffuses into a location with a different mean velocity and (ii) is then displaced from its initial position due to the mean velocity difference. Obviously, the displacement due to difference in the mean velocity will have a greater effect on the apparent diffusion than the diffusively induced random walk of the particles. With that picture in mind, the RMS displacement of the particle in the x-direction will be

$$\frac{\mathrm{d}\langle(\Delta x)^2\rangle^{1/2}}{\mathrm{d}t} \simeq \Delta u = \gamma\,\Delta y, \tag{5}$$

where Δu is the velocity difference due to the displacement, Δy, within the velocity gradient, γ. Now as Δy must have come about from diffusion:

$$\Delta y = (2D_{yy}\,t)^{1/2}. \tag{6}$$

Thus

$$\frac{\mathrm{d}\langle(\Delta x)^2\rangle^{1/2}}{\mathrm{d}t} = \gamma(2D_{yy}\,t)^{1/2} \rightarrow \langle(\Delta x)^2\rangle^{1/2} \sim t^{3/2}, \tag{7}$$

so that

$$\langle(\Delta x)^2\rangle \sim t^3, \tag{8}$$

i.e. the squared augmented displacement of the particles in the x-direction due to the mean shear field increases as t^3.

In the computer simulation, the measurement of the diffusion coefficients is accomplished by averaging the displacements of all of the particles in the simulation. The process is started by storing as reference points the positions of all of the particles in the simulation at the time that averaging begins. The simulation is stopped at intervals and an average is taken of the six independent correlations $\Delta x_i \Delta x_j$ over all of the particles in the simulation (here Δx_i represents the difference in the current x_i coordinate of the particle and its reference value). However, the item of interest is the distance that the particle has moved relative to the mean flow, hence, the reference point of each particle is moved along with the mean velocity appropriate to its position in the shear flow. Care must also be taken when a particle leaves through a periodic boundary of the control volume; there, the reference point must be moved a distance equal to the appropriate dimension of the control volume. A further correction is required for the D_{xx}-component which is augmented by the mean shear flow and hence will show the $(\Delta t)^3$ behaviour of equation (8). In that case, the effect of the mean flow may be removed by continuously subtracting the contribution from the mean velocity appropriate to the instantaneous position of the particle; this will be labelled as a 'corrected' value in the figures that are to follow.

This process yields the time history of the average value $\langle\Delta x_i \Delta x_j\rangle$. Figure 3 shows two examples of the average particle diffusion in the three principal directions, x, y and z, as a function of time. Figure 3(a) was computed for $\epsilon = 0.8$ and $\nu = 0.35$ while figure 3(b) was computed for the extreme case of $\epsilon = 0.4$ and $\nu = 0.05$. (While extreme in terms of the coefficient of restitution and concentration, the latter more clearly illustrates the split between the y- and z-directions, which is numerically apparent in the data but difficult to discern in figures of this type.) The figures are drawn on a log–log scale so that the power–law behaviour is reflected in the slopes of the lines. Consider, first of all, the diffusion history in the y- and z-directions. These demonstrate the behaviour expected from the above analysis. For short times, the line show a slope of 2:1, indicating that the displacement varies as the square of the time difference, $(\Delta t)^2$. For large Δt, the slope shallows until it varies linearly with Δt, as expected for a
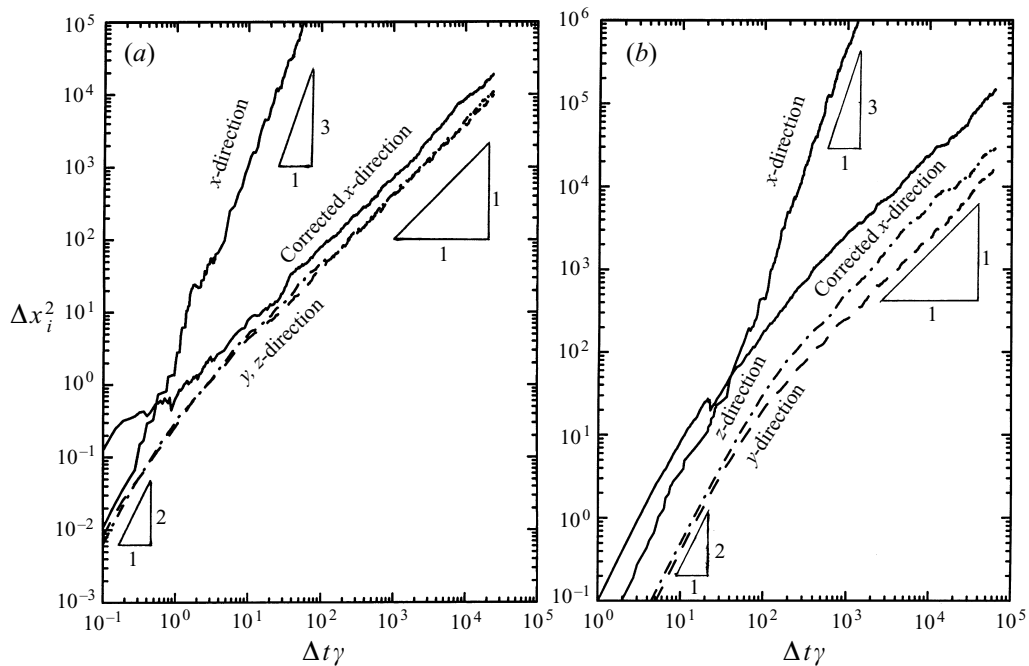
FIGURE 3. The diffusion history in the three normal directions, for (a) $\epsilon = 0.8$, $\nu = 0.35$, (b) $\epsilon = 0.4$, $\nu = 0.15$.
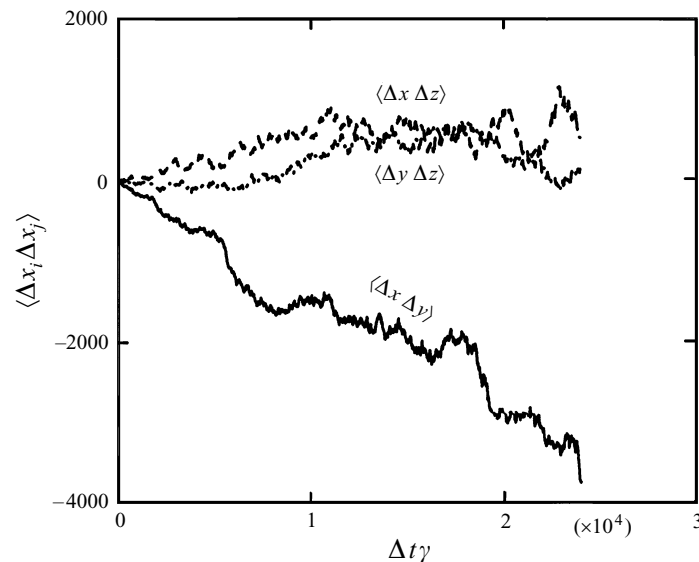

FIGURE 4. The diffusion history for the three off-diagonal correlations. The conditions are the same as for figure 3(a).

diffusive system. Two lines are plotted for the diffusion in the x-direction. The line labelled simply 'x-direction' measures the average x-direction displacement of the particles relative to a reference point moving with the velocity appropriate to its initial position in the shear flow; for large times, the line has a slope of 3:1, indicating that,
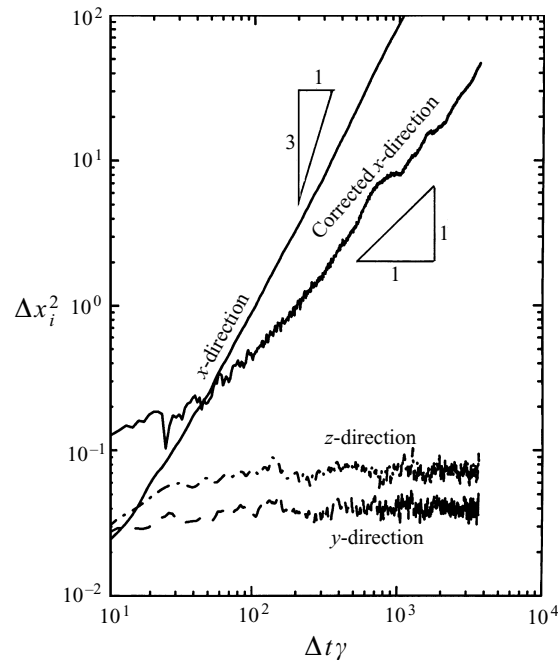
FIGURE 5. The diffusion history in the case where the particles have been trapped within a crystalline microstructure, for $\epsilon = 0.8$ and $\nu = 0.56$.

as predicted, the displacement grows with the cube of the time difference, Δt. However, if the displacement is corrected as described above, by continually subtracting the contribution from the local mean velocity, the 'corrected x-direction' varies linearly with Δt, in a manner similar to those for the y- and z-directions, indicating diffusive behaviour. Notice that the diffusion in the x-direction is always larger than that in the z-direction which is, in turn, larger than that in the y-direction. This was found to be always the case for all of the conditions in this study. However, the difference between the y- and z-direction diffusion is most evident at small densities and coefficients of restitution (this is why the $\epsilon = 0.4$ and $\nu = 0.05$ case was chosen for this figure) and the difference becomes insignificant at higher densities and coefficients of restitution. Figure 4 shows the other three correlations, $\langle \Delta x \Delta y \rangle$, $\langle \Delta x \Delta z \rangle$ and $\langle \Delta y \Delta z \rangle$, corresponding to the case shown in figure 3(a). Only one of these, $\langle \Delta x \Delta y \rangle$, is significant and has a negative slope. Collectively, this implies that there are only four non-zero components of the diffusion tensor, D_{xx}, D_{xy}, D_{yy} and D_{zz}.

Figure 5 shows a special case corresponding to $\epsilon = 0.8$ and $\nu = 0.56$. At such a large solids concentration the particles are locked into prismatic packing with which they were initially placed in the control volume. Thus, figure 5 does not represent a diffusive system. This can be clearly seen by examining the y-direction and z-direction lines which show that the displacement of the particles never exceeds more than a few tenths of a particle diameter. But, seemingly in contradiction to those observations, there does appear to be diffusion in the x-direction. However, from the nature of the microstructure described above, it is easy to see that this apparent diffusion is only superficial. Remember that the particles are arranged in strings oriented roughly in the x-direction. The shear rate is maintained by relative motion between the string and all the particles in a given string move with roughly the same velocity. But that velocity need not correspond exactly to that velocity appropriate to the position that a particle

instantaneously occupies in the shear flow. These small deviations accumulate to yield the apparent x-direction diffusion. A clue that something is wrong may be seen from the fact that the x-direction line has a slope slightly smaller than 3:1 and the corrected x-direction slope is slightly larger than 1:1. All of the data presented in this paper are carefully screened to exclude cases that show this kind of behaviour.

3.2. *Measurement by velocity correlation*

The diffusion coefficients may also be determined in a statistical manner without explicit particle tracking. The method used here is derived from Batchelor's (1949) extension of the method derived by Taylor (1922). The technique was originally developed to describe diffusion in stationary homogeneous turbulence. It is applicable to this situation as a uniform shear flow generates a spatially invariant granular temperature, so that, despite the inhomogeneity of the mean velocity field, the 'turbulence' field is homogeneous. Following Batchelor's analysis, one finds for large Δt

$$\langle \Delta x_i \Delta x_j \rangle = (\langle u_i'^2 \rangle \langle u_j'^2 \rangle)^{1/2} T_{Lij} \Delta t, \tag{9}$$

where, u_i' represents the instantaneous magnitude of the fluctuating velocity and T_{Lij} is the Lagrangian time scale:

$$T_{Lij} = \int_{-\infty}^{\infty} R_{Lij}(\xi)\, \mathrm{d}\xi, \tag{10}$$

where R_{Lij} is a scaled correlation of the instantaneous fluctuating particle velocities:

$$R_{Lij}(\xi) = \frac{\langle u_i'(t)\, u_j'(t+\xi) \rangle}{\langle u_i'^2 \rangle^{1/2} \langle u_j'^2 \rangle^{1/2}} \tag{11}$$

Note that, as it is assumed that the problem is statistically stationary, R_{Lij} should be independent of t. As a result, it is easy to see that $R_{Lij}(\xi) = R_{Lji}(-\xi)$.

The numerator in the definition of R_{Lij} is computed from taking the average of the correlations of instantaneous velocities of individual particles. At regular time intervals, usually spaced so as to be approximately one quarter of the average time between collisions for a particle, the instantaneous velocity of every particle in the system, minus the mean velocity appropriate to their position in the shear flow, is stored in a large array. (Shorter sampling intervals were used for the $\epsilon = 1.0$ data and longer sampling intervals were used for the $\epsilon = 0.4$ data as these showed very tightly peaked and broad correlations, respectively.) Once 1024 samples have been stored, the correlation for each particle is computed. This is accomplished by first taking the fast Fourier transform of the two components, multiplying the transform of one by the complex conjugate of the transform of the other and then performing a back transform, yielding the correlation function. Then, the correlation functions are averaged, first over every particle in the simulation, and secondly over each period at which a correlation is taken. Simpson's rule is then used to calculate the Lagrangian time scale T_L. By comparing (9) and (3) it can be seen that the magnitude of the diffusion coefficient is

$$D_{ij} = (\langle u_i'^2 \rangle \langle u_j'^2 \rangle)^{1/2} T_{Lij}. \tag{12}$$

An implication of (10), (11) and (12) is that there will always be a non-zero D_{ij} whenever the velocity correlation $\langle u_i u_j \rangle$ is non-zero. In other words, one can expect non-zero components of the diffusion tensor whenever there are non-zero components of the streaming part of the stress tensor. As Campbell (1989) has shown that, in a
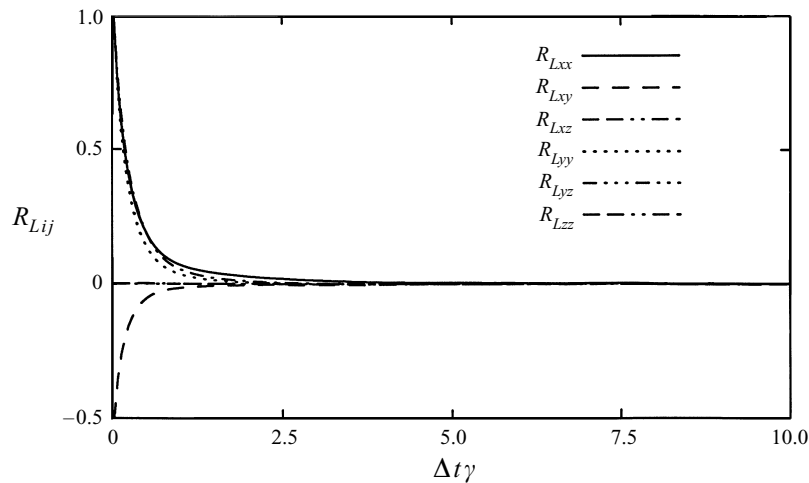
FIGURE 6. A typical example of the average velocity correlations, for $\epsilon = 0.8$ and $\nu = 0.35$. Note that only the positive-time portion of the correlations are shown.
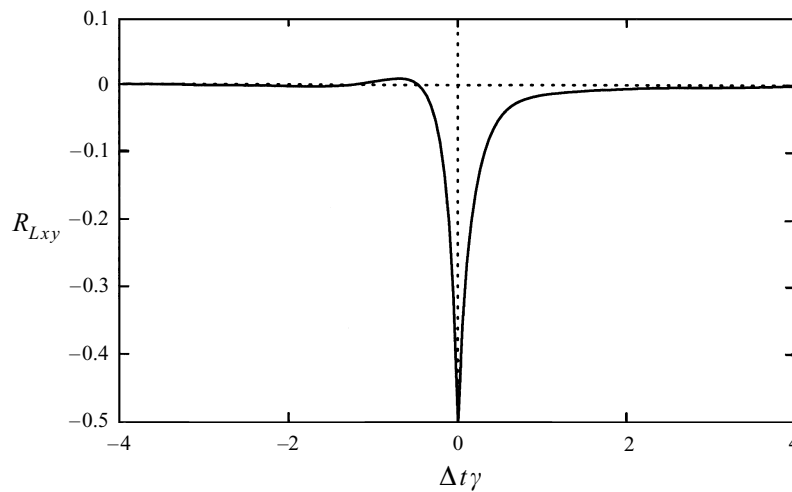

FIGURE 7. Measurements of R_{Lxy}. Notice that it is not an even function. This is for the case $\epsilon = 0.8$ and $\nu = 0.35$.

simple shear flow, there are no xz or yz stresses, streaming or otherwise, those components of the diffusion tensor should then be zero – exactly as was indicated by the particle tracking results.

Two typical examples of the resulting average correlation are shown in figure 6. This case was computed for the conditions $\epsilon = 0.8$ and at a solids concentration, $\nu = 0.35$. Plotted here are the traces for all six independent velocity correlations. It can be easily seen that the only non-zero components are the xx, xy, yy and zz ones. This should be expected as there will only be streaming stresses – and therefore only be velocity correlations – for those components (Campbell 1989). Furthermore, the diagonal components, xx, yy and zz, are positive while the xy component is negative. Lastly, it can be seen, just by visual observation, that the area under the R_{Lxx} curve is the largest, followed by that under the R_{Lyy} curve which is, in turn, followed by that under the R_{Lzz}
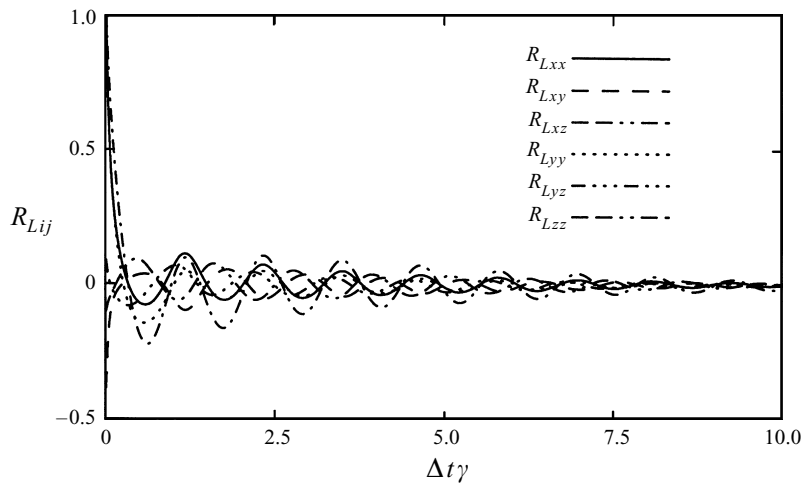
C. S. Campbell

FIGURE 8. An example of the velocity correlations in the case where the particles have been trapped within a crystalline microstructure, for $\epsilon = 0.8$ and $\nu = 0.56$. Note that only the positive-time portion of the correlations are shown.

curve. All of these observations correspond exactly with the particle tracking data shown above. The behaviour shown in figure 6 is pretty much what one would have expected. At zero Δt, the velocities of the particles are well correlated. However, after short periods of time, when the particles have experienced a few collisions, the resultant velocities lose all relationship to their former values and the correlation drops to zero. (In this figure, it appears to take somewhere of the order of 5 to 10 collisions before the correlation has completely disappeared.)

Figure 6 only shows the correlations for positive time displacements. This is perfectly fine for the diagonal components which must be even functions of Δt. (Taylor 1922 provides a proof for this, but it is easy to see that, since $R_{Lij}(\Delta t) = R_{Lji}(-\Delta t)$, the diagonal components, $i = j$, must be even functions.) However, the off-diagonal components need not be even. The corresponding correlation, $R_{Lxy}(\Delta t)$, is shown in figure 7 and is clearly not an even function.

Figure 8 shows the positive time correlations for the high-density case, $\nu = 0.56$. This is the figure corresponding to the particle tracking data shown in figure 5 and thus somewhat out of place in this paper as it does not represent a diffusive system. However, these correlations show an interesting decaying periodic structure that is absent from lower-concentration correlations such as those shown in figure 6. The period of the oscillation is approximately six average collision times per particle. This structure is a bit surprising since it indicates that the particles maintain some sort of memory of their previous velocities even after they have undergone many collisions. At first, it was thought that this structure was a relic of the use of periodic boundaries on the system. But then, the oscillation would be related to the time it takes a signal to propagate through the control volume and one would anticipate that the period would be somehow related to the linear dimensions of the control volume. Thus, tests were run on systems of various sizes, but no changes were observed in the periodic structure. Consequently, this periodic structure must be an indication of coordinated movement within the ordered microstructure into which the particles are formed. Apparently, the particles are following a coordinated pattern of collisions with their neighbours that persists over approximately a hundred collisions.
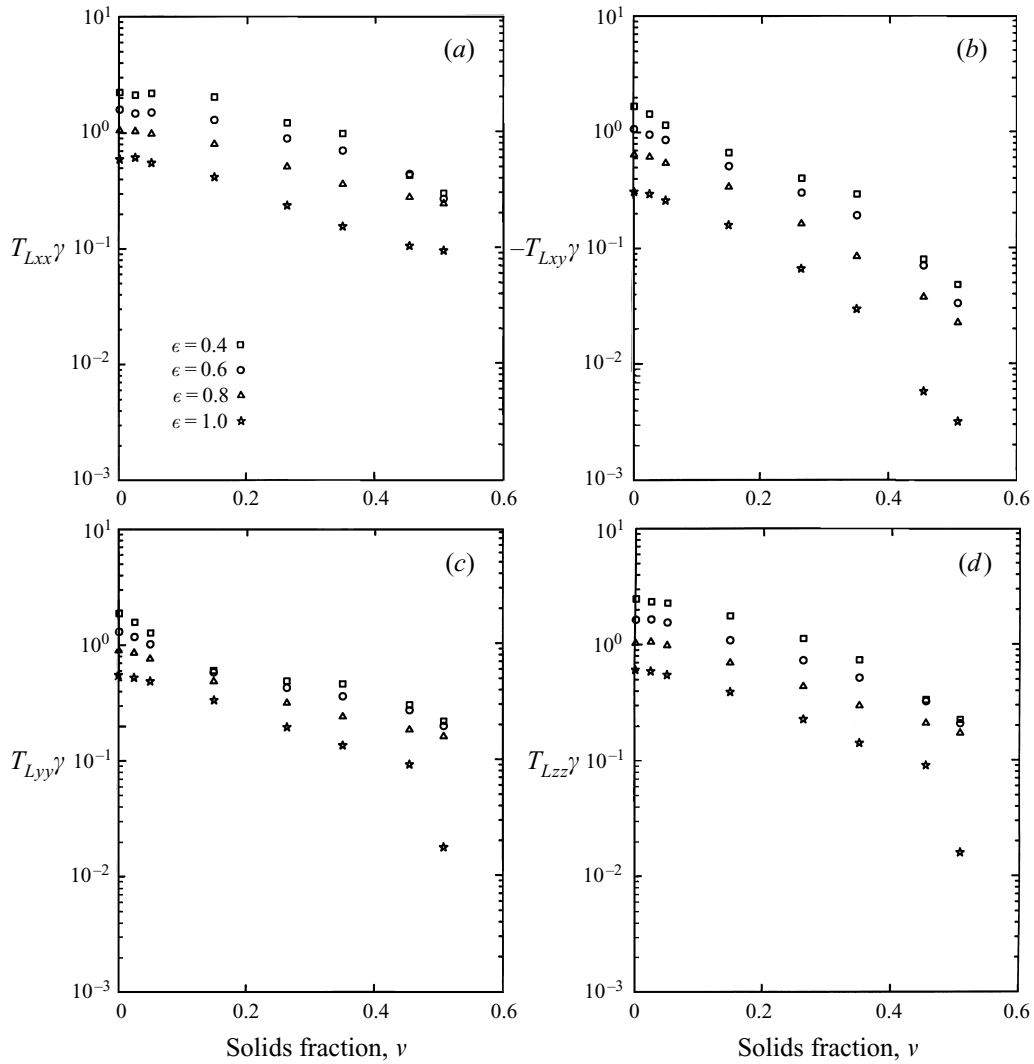
FIGURE 9. The components of the Lagrangian integral time-scale matrix: (a) T_{Lxx}, (b) T_{Lxy}, (c) T_{Lyy} and (d) T_{Lzz}.

Figure 9 shows plots of the four non-zero components of the Lagrangian integral time scale, T_{Lij}, scaled with the shear rate γ. (Note, that as T_{Lxy} is negative, its absolute value is plotted here.) The plots cover the full range of coefficients of restitution ($\epsilon = 0.4$, 0.6, 0.8 and 1.0 and concentrations ($\nu = 0.0001$, 0.025, 0.05, 0.15, 0.25, 0.35, 0.45, 0.50) that were considered in this study. (As is evident from figures 5 and 8, data were also accumulated for $\nu = 0.56$, but, as these have been shown to exhibit non-diffusive behaviour, they are excluded from this and subsequent figures.) Remember, that as defined in equation (6) T_L represents the integral under the corresponding correlation function, R_L. Consequently, the larger the value of T_L, the better correlated are the random velocities of the particles over longer time periods. Notice, first of all, that the values of T_L are monotonically decreasing functions of the solid fraction, ν. This probably should be expected as, the smaller the concentration, the longer the distance a particle travels between collisions, and, consequently, the longer the time

over which the velocities are well correlated. What might be surprising is that the drop is as small as it is. The value of T_L typically drops by a factor of about three between $\nu = 0.001$ and $\nu = 0.50$, a significantly smaller change than the factor of 120 drop in the mean spacing between the surfaces of particles. (Only the T_L component exhibits a change of that magnitude.) One might anticipate, from the discussions above, that T_L should be related to the collision time. But the collision time is a function both of the concentration and of the relative velocity between particles. But the relative velocity between particles is reflected in the granular temperature, which divergently approaches infinity as $\nu \to 0$. It appears then that, at small concentrations, the large interparticle velocities shorten the time between collisions at a rate that roughly balances the increase in time between collisions that is due to the increased interparticle spacing. Consequently, T_L is not dramatically changed.

For most of the range of solid fraction, T_L is a monotonically decreasing function of the coefficient of restitution, ϵ. Remember that ϵ is a measure of the inelasticity of collisions and that the smaller the value of ϵ, the greater the rate of energy dissipation during a collision. Consequently, the larger the coefficient of restitution the larger the granular temperature and the larger the granular temperature the larger the collision rate and the sooner the particle velocities become randomized. But, also, the more inelastic the collision, the weaker the collision impulse, the smaller the degree of velocity change imparted by the collision and the longer that a particle remembers its initial velocity. (This is apparent in the old freshman physics demonstration of colliding billiard balls. If the collision is elastic, the cue ball transfers all its momentum to its target and comes to a stop, losing all knowledge of its original state of motion. But if the collision is inelastic, the cue ball transfers only a portion of its momentum and will end up following its target, retaining a portion of its original velocity.) Thus, as one might have expected, with a small coefficient of restitution, more collisions are necessary to completely randomize the velocities.

3.3. *The diffusion tensor*

The preceding sections have described two independent methods for determining the diffusion coefficients and each provides an accuracy check on the other. The results for the four non-zero components of the diffusion tensor are plotted in figure 10. (As the D_{xy}-component is negative, its absolute value is plotted here.) The closed symbols represent the coefficients measured by particle tracking and the open symbols represent those computed from velocity correlations. The two methods agree within a few percent. As expected, the diffusion coefficients drop dramatically with increasing concentration, reflecting the effect of the decreased range of free motion and decreased granular temperatures on the diffusivity. Furthermore, the diffusivity is a generally decreasing function of the coefficient of restitution. This again should be expected as the larger the coefficient of restitution, the smaller the energy dissipation rate and the larger the granular temperature. There seem to be two exceptions to this rule. The first is in the D_{xx}- component, for which there seems to be very little effect of the coefficient of restitution on the results. The second is in the D_{xy}-component, for which the order appears to reverse, with the largest coefficients of restitution exhibiting the largest diffusivity at small concentrations and the smallest diffusivities at largest concentrations. The reason for this latter behaviour is not clear; however, it is not surprising given the wide spread of T_{Lxy} with ϵ that is apparent in figure 9(*b*).

As would be expected from the particle tracking data shown in figure 3 and the correlations shown in figure 6, the D_{xx}-component is larger than the D_{zz}-component which is, in turn, larger than the D_{yy}-component throughout the range of solids
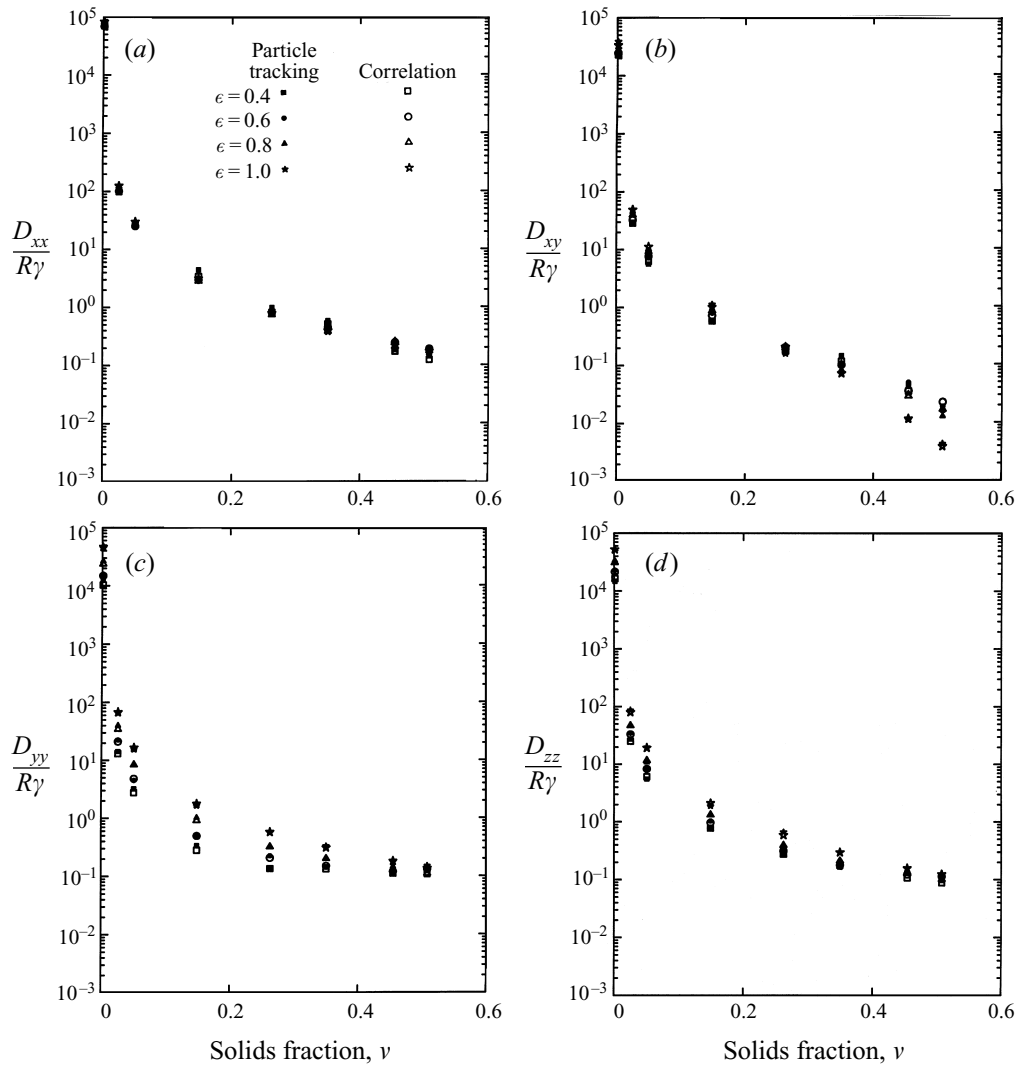
FIGURE 10. The components of the diffusion tensor: (*a*) D_{xx}, (*b*) D_{xy}, (*c*) D_{yy} and (*d*) D_{zz}.

concentration. (Furthermore, except at the largest concentrations, the values of D_{xy} are of roughly the same magnitude as D_{yy} and cannot be dismissed as insignificant.) The results of Campbell (1989) show that the anisotropy in the granular temperature mirrors that of the normal components of the diffusion tensor. This could explain the observed anisotropy as the diffusion coefficient should vary with the RMS random particle velocity, i.e. as the square root of the granular temperature. However, the same sort of anisotropy is apparent even when the coefficients are scaled by the square root of the appropriate granular temperature component. Thus, the diffusive anisotropy cannot be due solely to the anisotropy in the granular temperature and, perhaps, indicates some loosely organized internal structure that permits greater freedom of motion in the preferred directions. One might be able to intuitively understand how the shear flow might disrupt motion, at least in the *y*-direction. Diffusion of a particle in the *y*-direction places it in a region inhabited by other particles that possess relative velocity in the *x*-direction due simply to their position within the velocity gradient.

Such particles will have a larger collisional cross-section as this additional relative velocity allows them to cover a greater area perpendicular to the direction of diffusion during the time it takes the diffusing particle to pass their position. Remember that figure 2 shows that $S = 2R\gamma/T^{1/2}$ is of order one over most of the range of solid fraction. Consequently, the relative velocity due to the velocity gradient will be of the same order as that induced by the granular temperature which ultimately drives the diffusion process. Thus, the increased collisional cross-section, due to the relative velocity may significantly block diffusion in the y-direction. Such a process could explain how the shear motion itself induces some anisotropy into the diffusion tensor.

4. Conclusions

In the preceding sections, we have shown that a rapidly flowing granular material is a diffusive system except at large solids concentrations when the particles are trapped in a microstructure and prohibited from moving relative to their neighbours. Here, the particle diffusion is driven by the granular temperature in much the same way as the thermodynamic temperature causes diffusion of molecules. The diffusion coefficients were computed both by particle tracking and from the velocity correlations and both methods yield consistent answers. Particle tracking showed that the mean-squared displacement in the x-direction increased as the cube of the diffusion time – behaviour consistent with Taylor dispersion. However, if the diffusion velocities were instantaneously corrected for the changes in the mean velocity caused by changes in position within the mean shear flow, the diffusion in the x-direction exhibited normal diffusive behaviour.

The resulting diffusion was found to be anisotropic and, thus, cannot be described by a single diffusion coefficient. Instead, it must be described by a symmetric second-rank tensor of coefficients. Only four non-zero components, D_{xx}, D_{yy}, D_{zz} and D_{xy}, were found – which might be expected from the symmetries of the problem. The last, D_{xy}, indicated that gradient in the y-direction will induce a degree of diffusion in the negative x-direction (or vice versa). Furthermore, D_{xy} is of roughly the same magnitude as D_{yy} over most of the range of solid concentrations. Finally, over the range of conditions studied, the magnitude of the normal diffusion coefficients followed the pattern $D_{xx} > D_{zz} > D_{yy}$. This anisotropy could be partially, but not completely, attributed to a similar anisotropy in the granular temperature and it was speculated that the mean shear flow might, itself, introduce preferred diffusion directions.

REFERENCES

ALDER, B. J. & WAINWRIGHT, T. 1959 Studies in molecular dynamics. I. General method. *J. Chem. Phys.* **31**, 459–466.

BATCHELOR, G. K. 1949 Diffusion in a field of homogeneous turbulence: I. Eulerian analysis. *Austral. J. Sci. Res.* **2**, 437–450.

BRIDGWATER, J. 1980 Self-diffusion coefficients in deforming powders. *Powder Technol.* **25**, 129–131.

BUGGISH, H. & LÖFFELMANN, G. 1989 Theoretical and experimental investigation into local granular mixing mechanisms. *Chem. Proc. Engng* **26**, 193–200.

CAMPBELL, C. S., 1986 Computer simulation of rapid granular flows. *Proc. 10th US Natl. Cong. Applied Mechanics, Austin Texas, June 1986*, pp. 327–38. ASME.

CAMPBELL, C. S. 1989 The stress tensor for simple shear flows of a granular material. *J. Fluid Mech.* **203**, 449–473.

CAMPBELL, C. S. 1990 Rapid granular flows. *Ann. Rev. Fluid Mech.* **22**, 57–92.

CAMPBELL, C. S. 1993 Boundary interactions for two-dimensional granular flows. Part 1. Flat boundaries, asymmetric stresses and couple stresses. *J. Fluid Mech.* **247**, 111–136.

CAMPBELL, C. S. 1997 Computer simulation of powder flows. In *Powder Technology Handbook*, 2nd Edn. (ed. Gotoh), pp. 777–793. Dekker.

CAMPBELL, C. S. & ZHANG, Y. 1991 Granular shear flows: fluid-solid interfaces, impact strengths and self-diffusion. *Rep.* IFPRI.FN1. Department of Mechanical Engineering, University of Southern California.

CAMPBELL, C. S., ZHANG, Y. & CLEARY, P. 1991 Solidification, leading to clogging, in powder flows; also impact strengths and particle mixing in granular shear flows. *Rep.* IFPRI.2. Department of Mechanical Engineering, University of Southern California.

FAN, L. T. & CHEN, Y. 1990 Recent developments in solids mixing. *Powder Technol.* **61**, 255–287.

HEYES, D. M. 1986 The nature of extreme shear thinning in simple liquids. *Molecular Phys.* **57**, 1265–1282.

HSIAU, S. S. & HUNT, M. L. 1992 Experimental measurements of particle diffusion and velocity profiles in a granular-flow mixing layer. In *Advances in Micromechanics of Granular Materials – Proc. Second US/Japan Seminar on the Micromechanics of Granular Materials, Potsdam New York, August 5–9, 1991* (ed. H. H. Shen, M. Satake, M. Mehrabadi, C. S. Chang & C. S. Campbell), pp. 141–150. Elsevier.

LEES, A. W. & EDWARDS, S. F. 1972 The computer study of transport processes under extreme conditions. *J. Phys.* C: *Solid State Phys.* **5**, 1921–1929.

NATARAJAN, V. V. R., HUNT, M. L. & TAYLOR, E. D. 1995 Local measurements of velocity fluctuations and diffusion coefficients for granular material flow. *J. Fluid Mech.* **304**, 1–25.

POUX, M., FAYOLLE, P., BERTRAND, J., BRIDOUX, D. & BOUSQUET, J. 1991 Powder mixing: some practical rules applied to agitated systems. *Powder Technol.* **68**, 213–234.

SAVAGE, S. B. 1993 Disorder, diffusion and structure formation in granular flows. In *Disorder and Granular Media* (ed. D. Bideau & A. Hansen), pp. 255–285. Elsevier.

SAVAGE, S. B. & DAI, R. 1993 Studies of granular shear flows, wall slip velocities, layering and self-diffusion. *Mech. Mat.* **16**, 225–238.

SAVAGE, S. B. & JEFFREY, D. J. 1981 The stress tensor in a granular flow at high shear rates. *J. Fluid Mech.* **110**, 255–272.

SCOTT, A. M. & BRIDGWATER, J. 1976 Self-diffusion of spherical particles in a simple-shear apparatus. *Powder Technol.* **14**, 177–183.

TAYLOR, G. I. 1992 Diffusion by continuous movements. *Proc. Lond. Math. Soc.* (2), **20**, 196–212 (reprinted in *Scientific Papers* (ed. G. K. Batchelor), vol. II, pp. 172–184, Cambridge: Cambridge University Press, 1959).

TAYLOR, G. I. 1953 Dispersion of soluble matter in solvent flowing slowly through a tube. *Proc. R. Soc. Lond.* A **219**, 186–203.

TAYLOR, G. I. 1954a The dispersion of solid matter in turbulent flow through a pipe. *Proc. R. Soc. Lond.* A **223**, 446–468.

TAYLOR, G. I. 1954b Conditions under which dispersion of a solute in a stream of solvent can be used to measure molecular diffusion. *Proc. R. Soc. Lond.* A **225**, 473–477.

WANG, D. G. & CAMPBELL, C. S. 1992 Reynold's analogy for a shearing granular material. *J. Fluid Mech.* **244**, 527–546.

ZIK, O. & STAVANS, J. 1991 Self-diffusion in granular flows. *Europhys. Lett.* **16**, 255–258.